GEOPHYSICAL RESEARCH LETTERS, VOL. 27, NO. 3, PAGES 417-420, FEBRUARY 1, 2000

# Acoustic detection of immiscible liquids in sand

Jil T. Geller

Earth Sciences Division, Lawrence Berkeley National Laboratory, Berkeley, CA

Michael B. Kowalsky

Department of Civil and Environmental Engineering, University of California, Berkeley, CA

Patricia K. Seifert[1]

Department of Geology and Geophysics, University of California, Berkeley, CA

Kurt T. Nihei

Earth Sciences Division, Lawrence Berkeley National Laboratory, Berkeley, CA

**Abstract.** Laboratory cross-well P-wave transmission at 90 kHz was measured in a 61 cm diameter by 76 cm tall water-saturated sand pack, before and after introducing a non-aqueous phase organic liquid (NAPL) (n-dodecane). In one experiment, NAPL was introduced to form a lens trapped by a low permeability layer; a second experiment considered NAPL residual trapped behind the front of flowing NAPL. The NAPL caused significant changes in the travel time and amplitude of first arrivals, as well as the generation of diffracted waves arriving after the direct wave. The spatial variations in NAPL saturation obtained from excavation at the end of the experiment correlated well with the observed variations in the P-wave amplitudes and travel times. NAPL residual saturation changes of 4% were detectable and the 40 to 80% NAPL saturation in the NAPL lens was clearly visible at acoustic frequencies. The results indicate that small NAPL saturations may be more easily detected with amplitude rather than travel time data, but that the relationships between the amplitude changes and NAPL saturation may be more complex than those for velocity.

## 1. Introduction

Detecting and characterizing the distribution of immiscible liquids in unconsolidated sands is important for energy resource recovery and remediation of contaminated groundwater aquifers. Both petroleum products and organic liquid solvents are ubiquitous ground water contaminants that persist as non-aqueous phase liquids (NAPLs), owing to their low solubilities in water, and are source terms for extensive volatile organic chemical plumes. Seismic tomography may be an economically beneficial, non-invasive technique for mapping and monitoring the distribution of immiscible liquids between boreholes.

Significant changes in P-wave velocity and attenuation were measured in unconsolidated sand columns at 500 kHz for varying fractions of water and NAPLs [*Geller and Myer*, 1995]. *Geller and Myer* [1995] measured an approximately linear relationship between P-wave velocity and NAPL saturation and modeled it with simple mixing laws of the bulk-moduli of the liquid and solid phases [*Kuster and Toksöz*, 1974] for NAPLs of different densities and viscosities. However, the relationship between P-wave amplitudes and NAPL saturation was much more complex. The effect of the NAPL on amplitudes was consistently greater than the effect on velocity. Furthermore, while P-wave velocity was sensitive to the volume fraction of NAPL, amplitudes were also sensitive to its distribution.

For the case of homogeneously-distributed NAPL residual, *Seifert et al.* [1998] predicted measured velocity and amplitude changes by modeling one-dimensional scattering from stacks of water-NAPL-sand interfaces. However, this model under-predicted amplitude changes for heterogeneous, or patchy, NAPL distributions arising from unstable displacement conditions where NAPL flowed through the column in narrow channels (as opposed to a uniform front). Irregular NAPL distributions caused by flow instabilities and/or media heterogeneities are more representative of field conditions than homogeneous distributions. While the velocity trends are expected to be consistent at lower frequencies, amplitude changes may be strongly frequency-dependent. In this paper we describe a series of experiments conducted to measure the detectability of NAPLs by P-waves at a frequency range that is one order of magnitude lower than in the column studies. Experimental details beyond the scope of this paper are reported in *Geller et al.* [1999].

## 2. Description of Experiments

Two NAPL injection experiments were performed in a 61-cm diameter by 76-cm tall tank constructed of steel pipe with welded flanges and 25.4-mm aluminum top and bottom plates. The tank is lined with a 3-mm thick neoprene rubber jacket to accomodate confining pressures up to 0.5 MPa. Six 3-cm diameter acrylic wells are located just inside the vessel wall for the cross-well acoustic data acquisition. The top

[1]Now at McKinsey Corporation, Munich, Germany.



Paper number 1999GL010483.
0094-8276/00/1999GL010483$05.00

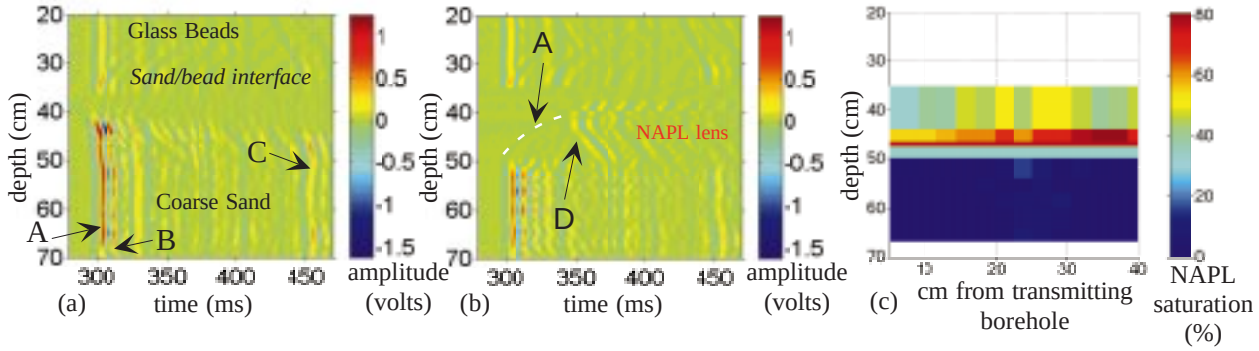


**Figure 1.** Results for Experiment A, detection of a NAPL lens. Depths are referenced from the top of the source borehole, which extends 11.4 cm from the top of the sandpack. (a) Zero offset scan of water-saturated sand. Arrows A, B and C indicate time of first arrival, reflection off tank wall adjacent to borehole and reflection off tank side, respectively. (b) Zero offset scan following the injection of n-dodecane. Arrow D indicates the second arrival. (c) NAPL saturation distribution in scanning plane from excavation.

and bottom plates of the tank have ports for fluid injection and drainage.

In each experiment, the tank was packed with well-sorted dry sand by pluviation from a constant height of fall and rate of flow. The packed tank was saturated with de-aired tap water injected from the tank bottom after flushing with carbon dioxide. n-Dodecane (DX2420-3, EM Science, Gibbstown, NJ) was injected from the bottom of the tank with a peristaltic pump (Masterflex console drive, pump 7021-24, Cole Parmer, Chicago, IL). n-Dodecane has a specific gravity of 0.745 and a viscosity slightly greater than water of 1.378 $kPa - s$ [*Riddick and Bunger*, 1970]. The acoustic velocity of n-dodecane is 1,290 m/s (22$^o$C) [*Wang and Nur*, 1991], which is 14% lower than that of water. By injecting from the bottom of the tank, buoyancy forces drive the lighter-than-water NAPL to channel upward, leaving residual NAPL segments along the flow paths. This distribution is analogous to the distribution created by the downward migration of denser-than-water NAPL contaminants in groundwater aquifers. Oil Red O dye (Sigma Chemical Co., St. Louis, MO) was added at 0.5 g/L to the NAPL to map its distribution after the experiment by excavation.

The cross-well seismic data is obtained using source and receiver tools mounted in acrylic tubes that are coupled to the borehole wall through a water annulus trapped between two O-rings. The rest of the borehole is kept dry to prevent the generation of borehole tube waves. The source is a bar piezoelectric crystal (PZT 5400 Navy I; resonance frequency 123 kHz) that is excited by a 90 kHz single-cycle tone amplified to 50 V peak-to-peak. This frequency produces P-wave wavelengths in the water-saturated sand of approximately 2 cm. The receivers are high frequency accelerometers (PCB 309A; resonance frequency >120 kHz) oriented horizontally in the scanning plane between boreholes. The received waveforms are preamplified by 40 dB, stacked 60 to 100 times and stored on the hard drive of a digital oscilloscope (LeCroy, LC334AM, Chestnut Ridge, NY). Scanning across the tank diameter between one pair of boreholes was performed manually before and after the NAPL injection by moving the source and receiver tools in vertical increments of 1 cm (approximately 1/2 wavelength).

At the end of the experiment, the three-dimensional distribution of the NAPL was measured by excavation. A thin-walled brass grid with 5×5×10 cm-deep cells covering the horizontal cross-sectional area of the tank was pressed into the sandpack. Samples of approximately 5 cm in depth were excavated consecutively from each cell. The NAPL volume in the samples taken from the scanning plane was measured by extracting the dyed NAPL into a known volume of clean n-dodecane and measuring the resulting dye concentration with a UV spectrophotometer (Hach DR/2000, Loveland, CO). The sand in each sample was oven dried and weighed to measure bulk porosity and to calculate the NAPL saturation.

Experiment A tested the acoustic response to the presence of a NAPL lens. The bottom 52.6 cm of the tank was packed with a coarse, sub-rounded 12/20 mesh (0.85 mm to 1.7 mm grain diameter) quartz sand (Unamin Corp., LeSuer, MN). A 25-cm thick layer of 44 to 88-micron diameter glass beads (MS-ML 105-53 glass-shot beads, Smith Industrial Supplies, San Lorenzo, CA) was placed over the sand to form a capillary barrier to the upward flowing NAPL and promote the formation of a NAPL lens within the coarse sand. No confining pressure was applied in this test. The NAPL was injected through a 7.3 cm diameter flow distribution disc at a height of 20 cm above the tank bottom. A total of 6.7 L of NAPL was injected at a flow rate of 94 mL/hr over 3 days. The fact that only water was collected from the top plate ports indicated that the capillary barrier kept all of the injected NAPL within the coarse sand.

Experiment B [*Kowalsky et al.*, 1998] measured the response to the presence of NAPL residual. The entire tank was packed with angular 12 mesh quartz sand (#2/12, RMC Lonestar, Pleasanton, CA). A confining pressure of 0.14 MPa was applied after the sand was water-saturated, while allowing the pore-water to drain. The packed tank porosity under confining pressure was estimated to be 0.3, based upon the mass of sand, the tank volume and the volume of water drained. The NAPL was injected through four 1.6-mm I.D. stainless steel tubes equally spaced 7.5 cm from the tank's vertical axis and approximately 20 cm from the tank bottom. After 2.5 hours of NAPL injection at 30 mL/hr, the NAPL broke through one of the three open ports on the tank top. This early breakthrough indicated that the NAPL flowed through one to several narrow channels. The flow rate was then increased to approximately 360 mL/hr to promote the development of additional NAPL flow paths. The injection was monitored from a fixed source and receiver location with time-lapsed, zero-offset, transmitted P-waves. The P-wave amplitudes decreased by approximately 35% during in-

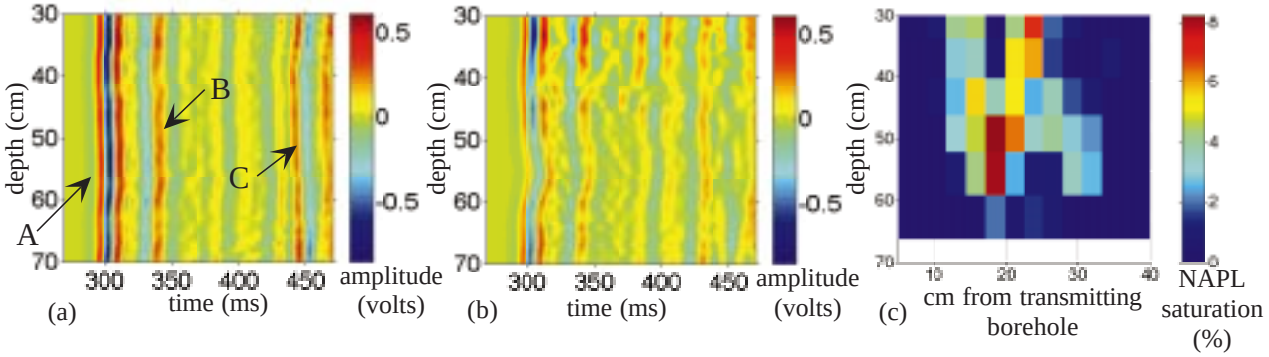


**Figure 2.** Results for Experiment B, detection of a NAPL residual. (a), (b) and (c) as in Figure 1.

jection and recovered to 23% of the baseline value after the injection stopped, presumably due to redistribution of the NAPL. The mass balance of NAPL injected into the tank and collected in the effluent indicated 595 mL of NAPL was trapped in the sand.

## 3. Results

In this paper, we report the zero-offset scans from the two experiments and the measured NAPL distributions. In zero-offset scans, the source and receiver are kept at equal depths as they are moved down the boreholes through the scanning region, therefore providing horizontally-averaged measurements. Tomographic inversion of the data sets to reveal both horizontal and vertical distributions of seismic attributes is ongoing and will be published separately. The results of two tomographic inversion methods have been reported to date using the data from Experiment B: straight-ray velocity tomography by *Kowalsky et al.* [1998] and asymptotic waveform inversion by *Keers et al.* [1999].

The zero-offset scans for Experiment A are shown in Figure 1. The first change in amplitude along the time axis is due to the first arrival of the P-wave (or travel time) and is indicated by arrow A in Figure 1(a). Two other arrivals, indicated with arrows B and C, are the back and side-wall reflections, respectively. The reference scan of the water-saturated tank in Figure 1(a) shows attenuation and diffraction due to the glass bead-sand interface. This interface is not sharp, and includes a transitional region of about two to three cm where the smaller diameter beads fill the pore space of the coarse sand.

In the post-injection scan (Figure 1b), neglibigle waveform changes occur in the glass bead layer. In the 15 cm below the glass bead layer, delayed travel times and amplitudes reductions of 60 to 95% indicate the presence of the NAPL lens. Below the lens, the residual NAPL produces amplitude reductions of 1 to 30% and changes in diffraction patterns. These waveform changes correspond to the NAPL saturation distribution in the scanning plane measured from the tank excavation shown in Figure 1(c). No NAPL was detected within the glass bead layer. Most of the NAPL accumulated in the top 15 cm of the coarse sand, where NAPL saturations ranged from 32% to 81% of the pore space. NAPL saturations are lower near the top of the lens (between depths 35 and 40 cm), because of the smaller pore sizes where smaller glass beads partially fill the coarse sand pores, then increase towards the middle of the lens, and decrease near the bottom. The layers of constant saturation at the bottom of the lens were measured by freezing with liquid nitrogen, without the brass grid, which facilitated the removal of large volumes of NAPL, but only provided average values over the horizontal cross-section of the tank. Below the lens, saturations range from 0 to 16%, with maximum values corresponding to the depths of maximum amplitude changes seen in Figure 1(b) at 58 and 63 cm.

The highly attenuated first arrivals within the lens are marked with a white line in Figure 1(b); the second arrivals are indicated by the arrow D. If the first arrivals are the direct arrivals, the decrease in travel time with depth below the lens as NAPL saturation decreases is consistent with relationships by *Geller and Myer* [1995]. However, the first arrivals may be head waves, diffracted into the faster, water-saturated media below the lens. If the second arrival is the direct arrival, the increasing travel time with depth may be due to variation in the ray path. The second arrival may, however, be a head wave traveling through the glass bead layer, which could produce the observed moveout, with relatively constant amplitude. Modeling to identify the direct arrivals and map ray paths is the subject of ongoing work and will be reported separately.

Figures 2(a) and (b) show the zero-offset scans for Experiment B, taken in the water-saturated sand before and following the injection of the NAPL, respectively. In the post-injection scan (Figure 2b), the presence of the NAPL causes changes in travel times, amplitudes and diffraction patterns (horizontal "v-shape" arrivals) throughout the depth of the tank. Before NAPL injection, travel times and amplitude (trough to peak) variations are ±0.2% and ±12%, respectively, without any systematic trend. After NAPL injection, the largest travel time increase of about 1.4% occurred at around 55 cm depth. The amplitude decreased by about 40% at around 40 cm depth and nearly 70% at the same elevation where the travel time increase was observed, which are significantly larger changes than the amplitude variability in the water-saturated sand.

Figure 2(c) shows the NAPL saturation distribution in the vertical cross-section between the scanning boreholes. Saturations range from 0.01% to 8.3%, with highest values occurring at the depths of maximum amplitude decrease in Figure 2(b). The horizontally-averaged saturation at this depth is 4.4%. The vertical discontinuity in the distribution is partially due to the three-dimensional geometry of the flow channels, which occur in and out of the plane of the cross-section.

## 4. Conclusions

The observed trends of the effect of NAPL on P-wave transmission at the tank-scale (acoustic frequencies) are consistent with behavior at the column scale (ultrasonic frequencies). Amplitude changes are significantly greater than velocity changes, and do not appear directly predictable from NAPL saturation alone. The mechanisms for amplitude changes in the tank experiments will be quantitatively explored in future work, however, the data reported here suggest that patchy NAPL distribution due to channelized flow may cause increased amplitude reduction when compared to the homogeneous distribution of immiscible phases, which is consistent with other observations and analyses of the effect of patchy fluid distribution [*Geller and Myer*, 1995; *Seifert et al.*, 1998; *Cadoret et al.*, 1998]. This form of attenuation is likely to be sensitive to the geometry of the scattering volumes, suggesting that scattering is still important at the lower frequencies of the tank-scale experiments, where the scale of liquid-phase heterogeneities is equivalent to, or greater than, the acoustic wavelength. NAPL residual saturation changes from NAPL flow channels of 4% (averaged over the presumed P-wave travel path) were detectable, and the 40 to 80% NAPL saturation in the NAPL lens was clearly visible at acoustic frequencies. Smaller NAPL saturations had a relatively larger effect on amplitudes at the tank scale compared to the column scale. This suggests that at the tank scale, propagating P-waves encounter a larger degree of heterogeneity in NAPL distribution compared to the column scale.

**Acknowledgments.** The authors would like to thank Larry Myer, John Peterson, Roland Gritto, and Henk Keers for insightful discussions, and the anonymous reviewers for helpful comments. This work was sponsored by the Director, Office of Energy Research, Office of Basic Energy Sciences, Geosciences Program, through U.S. Department of Energy contracts DE-AC03-76F00098 and DEF602-93ER14391 and by the Air Force Office of Scientific Research, USAF, under grant/contract number FQ8671-96-0-1169.

## References

Cadoret, T., G. Mavko and B. Zinszner, Fluid distribution effect on sonic attenuation in partially saturated limestones, *Geophysics 63,* 154-160, 1998.

Geller, J. T., M. B. Kowalsky, P. K. Seifert and K. T. Nihei, Acoustic detection of immiscible liquids in unconsolidated sand, *LBNL-42791*, 18 pp., Lawrence Berkeley National Lab., Berkeley, CA, 1999.

Geller, J. T. and L. R. Myer, Ultrasonic imaging of organic liquid contaminants in unconsolidated porous media, *Journal of Contaminant Hydrology, 19,* 85-104, 1995.

Keers, H., L. Johnson and D. Vasco, Crosswell imaging using asymptotic waveforms, *submitted to Geophysics,* 1999.

Kowalsky, M. B., J. T. Geller, P. K. Seifert, K. T. Nihei, R. Gritto, J. E. Peterson, Jr. and L. R. Myer, Acoustic visibility of immiscible liquids in poorly consolidated sand, *Proc. Soc. Exploration Geophysics,* 1041-1044, 1998.

Kuster, G. T. and Toksöz, M. N., Velocity and attenuation of seismic waves in two-phase media; Part I-Theoretical formulations, *Geophysics, 39,* 587-606, 1974.

Riddick, J. A. and Bunger, W. B., *Organic Solvents – Physical Properties and Methods of Purification,* 350 pp., Wiley-Interscience, New York, NY, 1970.

Seifert, P. K., J. T. Geller and L. R. Johnson, Effect of P-wave scattering on velocity and attenuation in unconsolidated sand saturated with immiscible liquids, *Geophysics, 63,* 161-170, 1998.

Wang, Z. and Nur, A., Ultrasonic velocities in pure hydrocarbons and mixtures, *J. Acoust. Soc. Am., 89,* 2725-2730, 1991.

J. T. Geller, K. T. Nihei, Earth Sciences Division, Lawrence Berkeley National Laboratory, Berkeley, CA, 94720 (e-mail: jtgeller@lbl.gov; ktnihei@lbl.gov)

M. B. Kowalsky, Department of Civil and Environmental Engineering, University of California, Berkeley, CA 94720 (e-mail: kowalsky@ccs.lbl.gov)

P. K. Seifert, McKinsey Corporation, Munich, Germany (e-mail: Patricia_Seifert@MCKINSEY.com)

(Received April 8, 1999; revised June 3, 1999;
accepted June 15, 1999.)